

A Novel Indicator to Predict the Onset of Instability of a Gravitational Flow on a Slope

^{1*}H. Chitsaz Boroujerdi; ²A. A. Bidokhti; ³Sh. Sharafatmandjoor

¹ Department of Oceanography, Graduate School of Marine Science and Technology, Science and Research Branch, Islamic Azad University, Tehran, Iran

² Institute of Geophysics, Tehran University, Tehran, Iran

³ Department of Mechanical and Aerospace Engineering, Science and Research Branch, Islamic Azad University, Tehran, Iran

Received 2 April 2012; revised 27 April 2012; accepted 12 May 2012

ABSTRACT: In order to present a quantitative indicator for the onset of instability, in this paper, the critical points of a stratified gravitational flow on a slope are found and analyzed. These points are obtained by means of the solution of the two-dimensional Navier-Stokes equations via the standard Arakawa-C finite-difference method. Results show that in the marginal Richardson numbers, the critical points begin to originate. Also, the cyclic evolution in the temporal differenced density field in the vicinity of the critical points is used as a quantitative criterion of the onset of mixing. Therefore, it is possible to predict the beginning of the mixing phenomenon via analysis of only a limited number of critical points.

Keywords: Gravitational Flow; Critical Points; Instability; Curvature Field

INTRODUCTION

Prediction of the instability of a moving stratified flow is a key element in the effective resolving of gravitational flows. For example, thermohaline circulation is extremely affected by the vertical mixing in a stratified flow. When the velocity difference across the interface between two fluids or two stratified layers are significant, the flow undergoes the Kelvin-Helmholtz instability. In gravitational flows where less dense fluid lays over the denser one, the onset of instability is given by the suitably defined Richardson number. It is well accepted that the layers will become unstable for Richardson numbers less than $Ri = 0.25$ (Drazin and Reid, 2004).

In practice, the statistical scaling and stability theories are applied to analyze the chaotic mixing systems (Sturman, 2006). Furthermore, some researchers have used the asymptotic directionality approach to deal with the geometry and topology of a chaotic mixing flow (Giona *et al.*, 2000). Since the mechanism of instability may comprise a broad range of behaviors from spatiotemporal chaos to full turbulence, the applied and quantitative decisive factors are of great utility.

On the other hand, followed by the multifractal analysis of the chaotic mixing (Ramshankar and

Gollub, 1991), one of the major findings in the field of spatiotemporal chaotic mixing has been the geometric method of Shinbrot and Ottino (Sturman, 2006) who presented the repeated stretching and folding of horseshoes as a model for mixing phenomenon. Moreover, Ottino presented the interesting kinematic feature of the two-dimensional flows that hyperbolic and elliptic points are created in strain-dominated and rotation-dominated regions respectively (Ottono and Khakhar, 2000).

Here, in order to introduce a quantitative criterion to predicting the onset of disordered instability, inspired by the geometric methods of (Sturman, 2006; Ramshankar and Gollub, 1991; Ouellette and Gollub, 2007), we focus on role of the critical points in the gravitational flows. In a typical gravitational flow, these pairs of critical points may emerge and annihilate. These mutual interactions have an essential effect on the dynamics of the flow. Specifically, we plan to show that the analysis of the scattering of just few critical points can be exploited as a quantitative criterion to predict the onset of instability.

MATERIALS AND METHODS

Governing equations and numerical methodology

The two-dimensional Navier-Stokes equations together with the Buoyancy equation are solved in the

*Corresponding Author Email: hchitsaz@srbiau.ac.ir

rotated coordinate system for the simulation of the dynamics of a gravitational flow with density stratification on a constant small slope surface with

consideration of the vertical slice assumption. The governing equations are

$$\frac{\partial u_r}{\partial t} + u_r \frac{\partial u_r}{\partial x_r} + w_r \frac{\partial u_r}{\partial z_r} = -\frac{1}{\rho_0} \frac{\partial(p+q)}{\partial x_r} + \sin(\gamma) \frac{\rho'}{\rho_0} g + \frac{\partial}{\partial x_r} \left(A_h \frac{\partial u_r}{\partial x_r} \right) + \frac{\partial}{\partial z_r} \left(A_z \frac{\partial u_r}{\partial z_r} \right), \quad (1)$$

$$\frac{\partial w_r}{\partial t} + u_r \frac{\partial w_r}{\partial x_r} + w_r \frac{\partial w_r}{\partial z_r} = -\frac{1}{\rho_0} \frac{\partial(p+q)}{\partial z_r} - \cos(\gamma) \frac{\rho'}{\rho_0} g + \frac{\partial}{\partial x_r} \left(A_h \frac{\partial w_r}{\partial x_r} \right) + \frac{\partial}{\partial z_r} \left(A_z \frac{\partial w_r}{\partial z_r} \right), \quad (2)$$

$$\frac{\partial \rho}{\partial t} + u_r \frac{\partial \rho}{\partial x_r} + w_r \frac{\partial \rho}{\partial z_r} = \frac{\partial}{\partial x_r} \left(K_h \frac{\partial \rho}{\partial x_r} \right) + \frac{\partial}{\partial z_r} \left(K_z \frac{\partial \rho}{\partial z_r} \right), \quad (3)$$

$$\frac{\partial u_r}{\partial x_r} + \frac{\partial w_r}{\partial z_r} = 0, \quad (4)$$

where u_r and w_r are respectively the velocity components parallel to the bed and normal to the bed, p is the hydrostatic pressure, q is the nonhydrostatic pressure, γ is the angle of rotation of the coordinate system, A_h and A_z are the horizontal and vertical eddy diffusivity coefficients respectively, ρ_0 is the reference density and K_h and K_z are the horizontal and vertical density diffusion coefficients respectively. The governing equations are solved using a finite-difference approach on an standard Arakawa-C grid with applying the successive-over-relaxation method for the solution of the Poisson equation for pressure. The finite-difference core of our solution is adopted from codes of (Kämpf, 2010). In this approach, a Cartesian grid is used for evaluating velocities. The grid points for pressures and densities are located midway between the velocity grid points. The rigid-lid assumption enables us to consider the undisturbed fluid surface aligned with vertical velocity grid points of the upper grid cells. We explicitly impose the no-penetration velocity boundary condition on the bed by defining the bottom topography via setting velocity values normal to solid boundaries to zero. As

we have used the regular structured grids, for general non-smoothed beds the boundaries are sharp and may not be expected to have accuracy of more than order one.

RESULTS AND DISCUSSION

In this study, the well-documented rectangular domain with initial density stratification is examined as a framework of the physical model for a gravitational flow facing instability and onset of mixing. The arrangement of the characteristics of the solution is explained in Fig. 1 and Table 1. Note that the prescribed CFL condition is fairly satisfied in all simulations.

As the simulation proceeds, for considerable density differences, the flow undergoes instability and therefore, the vertical dense layers begin the process of convective mixing. In longer times, the shear stresses originated from the bed cause the Kelvin-Helmholtz instability which is a set of counter-rotating vortices that move in the direction of the flow and interact with the previously existing vortices. The results are in good agreement with the existing literature (Ramshankar and Gollub, 1991).

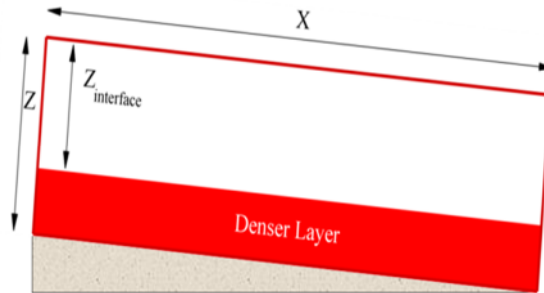


Fig. 1: Layout of the solution domain

Table 1: The solution configuration and the fluid properties.

Boundary conditions	
Top edge	Rigid-lid
Bottom edge	No-slip
Lateral edges	Periodic
Solution characteristics	
Extensions parallel and normal to the bed	$X = 101\text{ m}, Z = 31\text{ m}$
Grid spacings parallel and normal to the bed	$\Delta x = 5\text{ m}, \Delta z = 2\text{ m}$
Time integration interval	$\Delta t = 1\text{ s}$
Slope angle	$\gamma = 5^\circ$
Location of the density interface (see Fig. 1)	$z_{interface} = 3Z/4$
CFL condition	$\Delta t < \min\{\Delta x/u, \Delta z/w\}$
Fluid properties	
Reference density	$\rho_0 = 1028\text{ kg/m}^3$
Vertical and horizontal eddy diffusivity coefficients	$A_h = A_z = 10^{-3}\text{ m}^2/\text{s}$
Vertical and horizontal density diffusion coefficients	$K_h = K_z = 10^{-2}\text{ m}^2/\text{s}$

In order to investigate the critical points, the curvature field is analyzed. This field is evaluated using the Frenet relation $k = a_n u^{-2}$ where, a_n is the acceleration normal to the flow direction and u is the magnitude of the velocity vector. Note that a_n is computed by means of first-order time differencing of the velocity field with the time step of the simulation Δt .

Figs. 2a-b and c show the density difference ($\rho - \rho_0$), the stream function and the curvature fields for three different Richardson numbers after 6000s. In these experiments, all parameters except $\rho - \rho_0$ are kept fixed. The critical points are highlighted as the maxima of the curvature value contours. A couple of these points are schematically also marked in Fig. 2b by circles and plus indicators representing the elliptic and hyperbolic points respectively. As can be realized from Fig. 2, when the Richardson number is about 0.3, the mixing process is more likely diffusive and the curvature field contains only a weak set of maxima which are periodically repeated. In contrast, the velocity field does not notify the instability. Thus, one can use the curvature analysis as an indicator for the onset of instability.

As the Richardson number decreases to $Ri = 0.2$ the density field is triggered and the critical points in the

curvature field begin to spread while their vertical positions are scattered. This marginal Richardson number is consistent with the results of (Özgökmen et al., 2003). Note that the stream function field is still silent; revealing no information about the phenomenon. For lower Richardson number namely $Ri = 0.06$ the flow clearly goes through disordered convective mixing which is evident from the stream function and curvature fields.

Fig. 3 shows the values of the vertical component of the position of the critical points for different Richardson numbers. Vertical component of the position is chosen due to the periodicity of the boundary conditions in the lateral extension. One can anticipate that if the critical points are spread vertically, the vertical mixing is expected. The results show that at $Ri = 0.2$ the diversity of the vertical positions is remarkable. Table 2 brings an overview of the issue in terms of standard deviation of the vertical component of the position of the critical points. The maximum deviation corresponding to $Ri = 0.2$ could be a sign of incept of instability process. This outcome matches with the qualitative description that the flow experiences vigorous stretching and rotation in hyperbolic and elliptic points respectively (Sturman, 2006).

A Novel Indicator to Predict the Onset of Instability

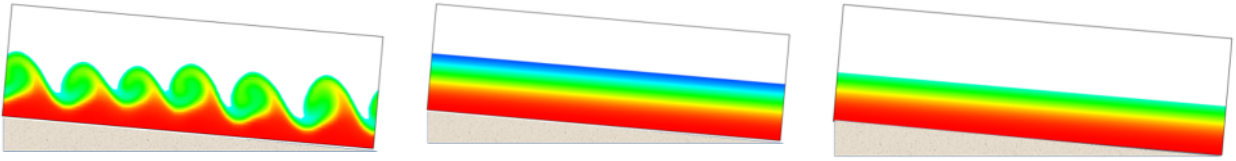


Fig. 2a: Contours of density difference $\rho - \rho_0$ at 6000 s from left to right for: $Ri = 0.06, 0.2$ and 0.3 . Small values are brought colorless.

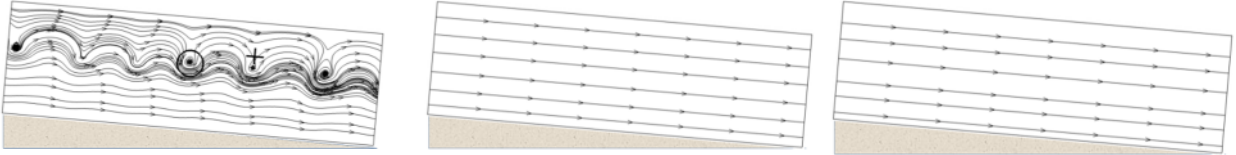


Fig. 2b: The stream function field at 6000 s from left to right for: $Ri = 0.06, 0.2$ and 0.3 . Sample elliptic and hyperbolic points are shown by circles and plus signs respectively.

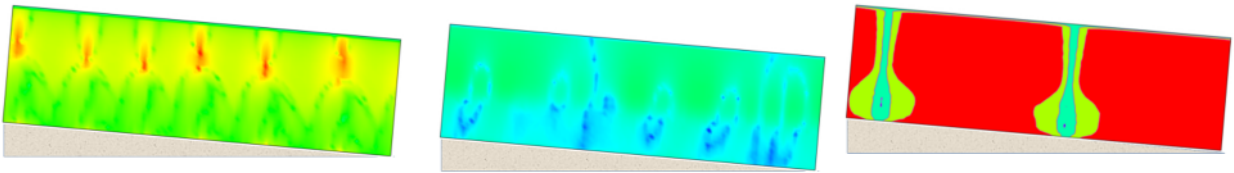


Fig. 2c: Contours of curvature at 6000 s from left to right for: $Ri = 0.06, 0.2$ and 0.3 . The maxima of this field correspond to critical points.

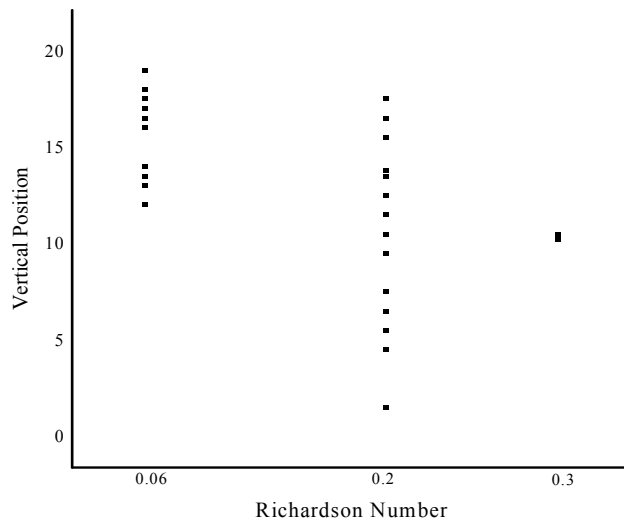


Fig.3: The vertical position of the critical points at 6000 s for different Richardson numbers.

Table 2: Standard deviation of the vertical positions of the critical points at 6000 s.

Richardson number	0.3	0.2	0.06
Standard deviation	0.15	4.45	2.24

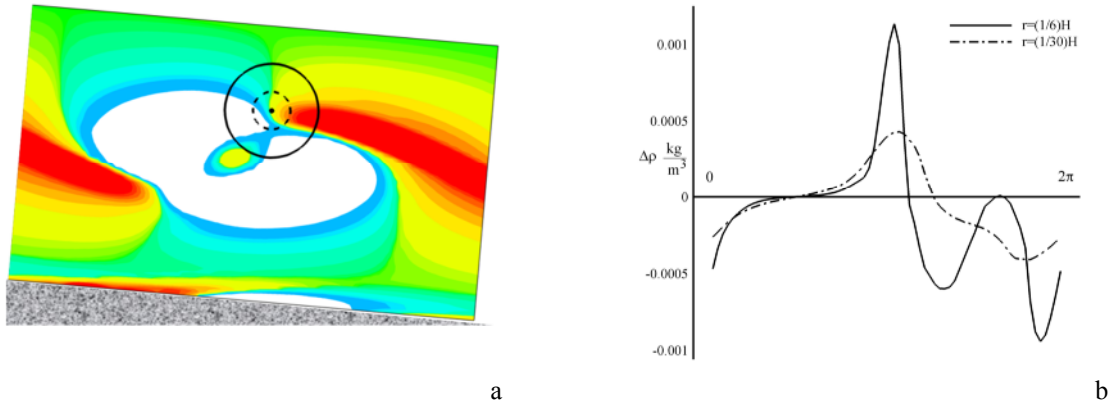


Fig.4, a: Contours of the temporal differenced density at 4000 s. Values less than $0.002\text{kg}/\text{m}^3$ are brought colorless for more clarity, b: Values of the temporal differenced density on circles of the left panel with respect to the sampling angle.

Now, in order to more deeply analyze the effect and role of the critical points, we concentrate on the evolutions adjacent to the critical points. In Fig.4a, the time differenced density field for another experiment with extensions (81×51) is shown at 4000 s. One can see that around the critical points which are indicated by the filled circles, a cyclic evolution in the temporal difference values is evident. This issue can be verified by reporting their discretized values on concentric circles with radii $r = \left(\frac{1}{6}\right)H, r = \left(\frac{1}{30}\right)H$ where H is the extent normal to the flow surface.

In Fig. 4b the temporal difference values of the density corresponding to these circles are revealed. The figure confirms that the interval of variation of the temporal difference values is bracketed between two equal values with different sizes. This special condition is not the case in other regions of the field. Furthermore, one can observe that the mentioned critical points are located at the mixing front of the flow.

This phenomenon can be expressed as follows. Since the velocity values vanish at the critical points, considerable gradients are produced around them. Therefore, emergence and annihilation of the critical points are key mechanisms in the mixing of dense layers. It should be remarked that the most effective cause of the mixing phenomenon is the convection which is governed by the velocity magnitude.

CONCLUSION

We presented a sensitive pointer for the onset of instability in gravitational flows. The results show that there exist a direct relation between the divergence of the critical points and the mixing rate in a gravitational flow on a slope. On the other hand,

considering the cyclic evolution in the temporal density difference field, one can conclude that in the vicinity of the critical points, oscillations with identical amplitude but with opposite signs occur in the field. Such a pointer can be a novel basis for the tracking and detection of locations where mixing originates in a gravitational flow.

REFERENCES

- Drazin, P.G.; Reid, W.H., (2004). Hydrodynamic Stability, 2nd Ed. Cambridge University Press.
- Giona, M.; Adrover, A.; Muzzio, F.J.; Cerbelli, S., (2000). The geometry of mixing in 2D time-periodic chaotic flows, Chem. Eng. Sci. 55, 381-389.
- Kämpf, J., (2010). Advanced Ocean Modelling Using Open-source Software, Springer-Verlag Berlin Heidelberg.
- Ottino, J.M.; Khakhar, D.V., (2000). Mixing and segregation of granular materials, Annu. Rev. Fluid Mech. 32:55-91
- Ouellette, N.T.; Gollub, J.P., (2007) Curvature fields, topology, and the dynamics of spatiotemporal chaos, Phys. Rev.Lett., PRL 99,194502.
- Ouellette, N.T.; Gollub J. P., (2008) Dynamic Topology in Spatiotemporal Chaos, Phys. Fluids, 20, 064104.
- Özgökmen, T.M.; Johns, W.E.; Peters, H.; Matts, S., (2003) Turbulent mixing in the red sea outflow plume from a high-resolution nonhydrostatic model, J. Phys. Oceanogr., 33, 1846-1869.
- Ramshankar, R.; Gollub, J. P., (1991) Transport by capillary waves, Part II. Scalar dispersion and the structure of the concentration field, Phys. Fluids A., 3, 1344-1350.
- Sturman, R.; Ottino, J.M.; Wiggins, S., (2006). The mathematical foundations of mixing, Cambridge University Press.

How to cite this article: (Harvard style)

Chitsaz Boroujerdi, H.; Bidokhti, A. A.; Sharafatmandjor, SH., (2013). A Novel Indicator to Predict the Onset of Instability of a Gravitational Flow on a Slope. Int. J. Mar. Sci. Eng., 3 (2), 85-90.